DESY 12-207

One-loop effects on MSSM parameter determination via chargino production at the LC

Aoife Bharucha[*,1], Jan Kalinowski[†,2], Gudrid Moortgat-Pick[‡,1,3], Krzysztof Rolbiecki[§,3,4] and Georg Weiglein[¶,3]

[1] *II. Institut für Theoretische Physik, University of Hamburg, Luruper Chaussee 149, D-22761 Hamburg, Germany*

[2] *Faculty of Physics, University of Warsaw, 00681 Warsaw, Poland*

[3] *DESY, Deutsches Elektronen-Synchrotron, Notkestr. 85, D-22607 Hamburg, Germany*

[4] *Instituto de Física Teórica, IFT-UAM/CSIC, 28049 Madrid, Spain.*

Abstract

At a future linear collider very precise measurements, typically with errors of $< 1\%$, are expected to be achievable. Such an accuracy gives sensitivity to the quantum corrections, which therefore must be incorporated in theoretical calculations in order to determine the underlying new physics parameters from prospective linear collider measurements. In the context of the chargino–neutralino sector of the minimal supersymmetric standard model, this involves fitting one-loop predictions to prospective measurements of the cross sections, forward-backward asymmetries and of the accessible chargino and neutralino masses. Taking recent results from LHC SUSY and Higgs searches into account we consider three benchmark scenarios, each with characteristic features. Our analysis shows how an accurate determination of the desired parameters is possible, providing in addition access to the stop masses and mixing angle.

[*]aoife.bharucha@desy.de
[†]jan.kalinowski@fuw.edu.pl
[‡]gudrid.moortgat-pick@desy.de
[§]krzysztof.rolbiecki@desy.de
[¶]georg.weiglein@desy.de

1 Introduction

A linear collider (LC) [1–3] will be an ideal environment for high precision studies of physics beyond the standard model (BSM). A particularly well-motivated BSM theory is the Minimal Supersymmetric Standard Model (MSSM). This provides the lightest neutralino as a candidate to explain the evidence for WIMP-like dark matter in the universe [4, 5]. Further, naturalness arguments (see e.g. ref. [6]) support light higgsino-like charginos and neutralinos, as also predicted by GUT motivated SUSY models [7]. The charginos and neutralinos could therefore be within reach of a first stage linear collider.

In order to precisely determine the nature of the underlying SUSY model, the fundamental parameters have to be determined in the most model-independent way possible. The determination of the U(1) parameter M_1, the SU(2) parameter M_2, the higgsino parameter μ and $\tan\beta$, the ratio of the vacuum expectation values of the two neutral Higgs doublet fields, at the percent level via chargino and neutralino pair-production has been shown to be possible at LO (see ref. [8] and references therein). Due to the expected high precision of mass and coupling measurements at the LC, as well as the fact that one-loop effects in the MSSM are often large, higher order effects have to be considered. Taking these corrections into account additional MSSM parameters become relevant, such as the masses of the stops and sleptons, which are also so far weakly constrained by the LHC.

In this paper we show how it would be possible to determine the fundamental parameters of the chargino and neutralino sector at the LC, including the uncertainty arising due to higher order effects. Specifically, we calculate the next-to-leading order (NLO) corrections to the cross-section (σ) and forward-backward asymmetry (A_{FB}) for chargino production, and also to the chargino and neutralino masses. A number of next-to-leading order (NLO) calculations of chargino and neutralino pair production at the LC can be found in the literature [9–12]. We perform our calculations in the on-shell (OS) scheme such that, as far as possible, the physical interpretation of the masses is clear. Recent work on the OS renormalization of the chargino-neutralino sector can be found in refs. [13–16].

By fitting experimental results to these loop corrected predictions we show that it is possible to extract the fundamental parameters of the MSSM Lagangian. However due to the greater number of parameters, performing the fit is more involved as for the LO analysis. Choosing three potential MSSM scenarios, we assess the impact of the loop corrections and the feasibility of such an extraction in each. We further investigate the impact of obtaining masses of the charginos and neutralinos from threshold scans rather than the

continuum (see ref. [1]) on the resulting accuracy of the parameters obtained from the fit.

The paper is organised as follows. In sec. 2 we introduce the process studied and define necessary notation. We then provide details of the calculation of the loop corrections in sec. 3, including details of the renormalization scheme used. In sec. 4 we further discuss the method employed in order to fit to the MSSM parameters, define the scenarios considered, and present our results. Finally in sec. 5 we discuss the implications of the results of the fits.

2 Process studied and tree-level relations

In this paper we study the determination of the fundamental parameters in the chargino–neutralino sector of the MSSM, via chargino production at a LC. The charginos, $\tilde{\chi}^{\pm}$, and neutralinos, $\tilde{\chi}^0$, are the mass eigenstates of the gauginos and higgsinos, as seen from the relevant part of the MSSM Lagrangian [17],

$$\begin{aligned}\mathcal{L}_{\tilde{\chi}} =& \overline{\tilde{\chi}_i^-}(\not{p}\delta_{ij} - P_L(U^* X V^\dagger)_{ij} - P_R(V X^\dagger U^T)_{ij})\tilde{\chi}_j^- \\ &+ \frac{1}{2}\overline{\tilde{\chi}_i^0}(\not{p}\delta_{ij} - P_L(N^* Y N^\dagger)_{ij} - P_R(N Y^\dagger N^T)_{ij})\tilde{\chi}_j^0, \end{aligned} \tag{1}$$

where $P_{L/R} = 1/2(1 \mp \gamma_5)$. The mass matrix for the charginos is given by

$$X = \begin{pmatrix} M_2 & \sqrt{2} M_W s_\beta \\ \sqrt{2} M_W c_\beta & \mu \end{pmatrix}, \tag{2}$$

where $s_\beta/c_\beta = \sin\beta/\cos\beta$, and M_W is the mass of the W boson. This matrix is diagonalised via the bi-unitary transformation $\mathbf{M}_{\tilde{\chi}^+} = U^* X V^\dagger$, where U and V are complex unitary matrices. The mass matrix for the neutralinos in the $(\tilde{B}, \tilde{W}, \tilde{H}_1, \tilde{H}_2)$ basis is given by

$$Y = \begin{pmatrix} M_1 & 0 & -M_Z c_\beta s_W & M_Z s_\beta s_W \\ 0 & M_2 & M_Z c_\beta c_W & -M_Z s_\beta c_W \\ -M_Z c_\beta s_W & M_Z c_\beta c_W & 0 & -\mu \\ M_Z s_\beta s_W & -M_Z s_\beta c_W & -\mu & 0 \end{pmatrix}, \tag{3}$$

where $s_W(c_W)$ is the sin(cos) of the electro-weak mixing angle θ_W. Since Y is complex symmetric, its diagonalisation requires only one unitary matrix N, via $M_{\tilde{\chi}^0} = N^* Y N^\dagger$.

We study the pair production of charginos, $\tilde{\chi}_1^-$,

$$e^+ e^- \to \tilde{\chi}_1^+ \tilde{\chi}_1^-, \tag{4}$$

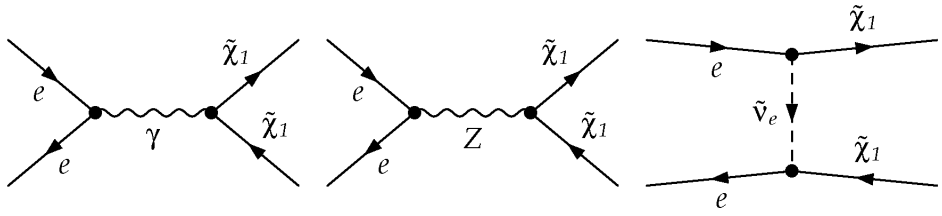

Figure 1: Tree-level diagrams for the production of charginos $\tilde{\chi}_1^+$ and $\tilde{\chi}_1^-$ at the LC.

including effects due to polarised beams. Neglecting the electron-Higgs couplings, this process occurs at leading order via three diagrams, as seen in fig. 1.

The transition matrix element can be written as [18],

$$\mathcal{M}_{\alpha\beta}(e^+e^- \to \tilde{\chi}_i^+\tilde{\chi}_j^-) = \frac{e}{s} Q_{\alpha\beta} \left[\bar{v}(e^+)\gamma_\mu P_\alpha u(e^-)\right] \left[\bar{u}(\tilde{\chi}_j^-)\gamma^\mu P_\beta v(\tilde{\chi}_i^+)\right], \quad (5)$$

where $Q_{\alpha\beta}$ denotes the bilinear charges, $\alpha = L, R$ refers to the chirality of the e^+e^- current and $\beta = L, R$ to that of the $\tilde{\chi}_i^+\tilde{\chi}_j^-$ current. The summation over α and β is implied. The bilinear charges are comprised of the propagators and couplings

$$\begin{aligned}
Q_{LL} &= C^L_{\tilde{\chi}_i^+\tilde{\chi}_j^-\gamma} - D_Z G_L C^L_{\tilde{\chi}_i^+\tilde{\chi}_j^- Z}, \\
Q_{RL} &= C^L_{\tilde{\chi}_i^+\tilde{\chi}_j^-\gamma} - D_Z G_R C^L_{\tilde{\chi}_i^+\tilde{\chi}_j^- Z}, \\
Q_{LR} &= C^R_{\tilde{\chi}_i^+\tilde{\chi}_j^-\gamma} + D_Z G_L \left(C^R_{\tilde{\chi}_i^+\tilde{\chi}_j^- Z}\right)^* + \frac{i}{2\,e} D_{\tilde{\nu}} \left(C^R_{\tilde{\nu}_e e^+\tilde{\chi}_i^-}\right)^* C^R_{\tilde{\nu}_e e^+\tilde{\chi}_j^-}, \\
Q_{RR} &= C^R_{\tilde{\chi}_i^+\tilde{\chi}_j^-\gamma} + D_Z G_R \left(C^R_{\tilde{\chi}_i^+\tilde{\chi}_j^- Z}\right)^*,
\end{aligned} \quad (6)$$

for which the required MSSM couplings for the $\tilde{\chi}_i^+\tilde{\chi}_j^-\gamma$, $\tilde{\chi}_i^+\tilde{\chi}_j^- Z$ and $e\tilde{\nu}_e\tilde{\chi}_i^+$ vertices are given by

$$\begin{aligned}
C^{L/R}_{\tilde{\chi}_i^+\tilde{\chi}_j^-\gamma} &= ie\delta_{ij}, \\
C^L_{\tilde{\chi}_i^+\tilde{\chi}_j^- Z} &= -\frac{ie}{c_W s_W}\left(s_W^2\delta_{ij} - U^*_{j1}U_{i1} - \frac{1}{2}U^*_{j2}U_{i2}\right), \\
C^R_{\tilde{\chi}_i^+\tilde{\chi}_j^- Z} &= C^L_{\tilde{\chi}_i^+\tilde{\chi}_j^- Z}(U \to V^*), \\
C^R_{\tilde{\nu}_e e^+\tilde{\chi}_i^-} &= -\frac{ie}{s_W} V_{i1},
\end{aligned} \quad (7)$$

and G_L, G_R, D_Z and $D_{\tilde{\nu}}$ are defined via

$$G_L = \frac{s_W^2 - \frac{1}{2}}{s_W c_W}, \qquad G_R = \frac{s_W}{c_W},$$
$$D_Z = \frac{s}{s - M_Z^2}, \qquad D_{\tilde{\nu}} = \frac{s}{t - m_{\tilde{\nu}}^2}. \tag{8}$$

In the equations above, e denotes the electric charge, m_e and M_Z are the masses of the electron and Z boson. D_Z and $D_{\tilde{\nu}}$ refer to the propagators of the Z boson and sneutrino (of mass $m_{\tilde{\nu}}$), in terms of the Mandelstam variables s and t. We can neglect the non-zero Z boson width for the considered energies.

One can therefore express the transition matrix element in terms of M_2, μ and $\tan\beta$, in addition to the known SM parameters. However, the expected accuracy of the measurements at the linear collider is such that one-loop corrections become relevant, and we shall see in the following section how the higher order expressions depend on many additional MSSM parameters.

3 NLO contributions and renormalization

We have calculated the full one-loop corrections to the process $e^+e^- \to \tilde{\chi}_1^+\tilde{\chi}_1^-$, following ref. [19], within the complex MSSM; examples for the contributing self-energy, vertex and box diagrams are shown in fig. 2. For the calculation we have used the program `FeynArts` [20–24], which allowed an automated generation of the Feynman diagrams and amplitudes. Together with the packages `FormCalc` [25–27] and `LoopTools` [25] we derived the final matrix elements and loop integrals. We assume a unit CKM matrix. We regularise using dimensional reduction [28–30], which ensures that SUSY is preserved, via the implementation described in refs. [25, 31]. In order to obtain finite results we calculated the counterterms for the involved 2- and 3-point vertices, according to the renormalization scheme outlined below, and implemented these in the model files of `FeynArts`.

A number of one-loop calculations in the gaugino-higgsino sector can be found in the literature, mainly in the CP-conserving MSSM [9, 32–40], but some of which apply a renormalization scheme that is also applicable for complex parameters [9,38]. CP-odd observables have also been calculated at the one-loop level, for instance in refs. [41–43], but no dedicated renormalization scheme was required in these cases as the observables studied were UV-finite. Since we intend to extend the current study to the case of complex parameters, here we follow the approach of refs. [14, 19] closely, where a dedicated on-shell renormalization scheme for the chargino and neutralino

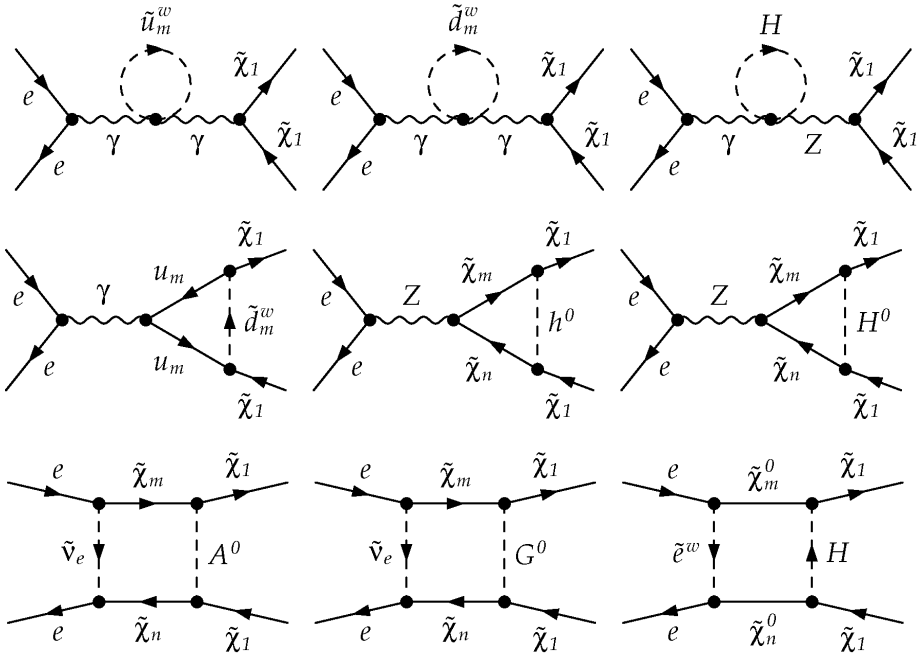

Figure 2: Examples of one-loop self-energy (upper), vertex (middle) and box (lower) diagrams for the production of charginos $\tilde{\chi}_1^+$ and $\tilde{\chi}_1^-$ at the LC.

sector of the MSSM with complex parameters was developed. In the following we will therefore only discuss the parameter renormalization of the chargino and neutralino sector briefly, and for further details about the chargino field renormalization and the renormalization of other sectors we refer the reader to refs. [14, 15, 19, 44].

The mass matrix in the chargino sector, eq. (2), is renormalized via

$$X \to X + \delta X, \tag{9}$$

where δX is defined by

$$\delta X = \begin{pmatrix} \delta M_2 & \sqrt{2}\delta(M_W s_\beta) \\ \sqrt{2}\delta(M_W c_\beta) & \delta\mu \end{pmatrix}, \tag{10}$$

containing the renormalization constants δM_2 and $\delta\mu$, as well as renormalization constants (RCs) from other sectors, δc_β, δs_β (which can be expressed in terms of $\delta \tan\beta$), and δM_W, defined in ref. [19]. The neutralino mass matrix, eq. (3), is similarly renormalized via

$$Y \to Y + \delta Y, \tag{11}$$

where δY is defined analogously to δX in eq. (10) and contains the additional δM_1, cf. eq. (3).

Following e.g. ref. [14], δM_1, δM_2 and $\delta\mu$ are determined by choosing three out of the total six physical masses of the charginos and neutralinos to be on-shell, i.e. the tree-level masses, $m_{\tilde{\chi}_i}$, coincide with the one-loop renormalized masses, $M_{\tilde{\chi}_i} = m_{\tilde{\chi}_i} + \Delta m_{\tilde{\chi}_i}$,

$$\begin{aligned}\Delta m_{\tilde{\chi}_i} \equiv & -\frac{m_{\tilde{\chi}_i}}{2}\mathrm{Re}[\hat{\Sigma}^L_{ii}(m^2_{\tilde{\chi}_i}) + \hat{\Sigma}^R_{ii}(m^2_{\tilde{\chi}_i})] - \frac{1}{2}\mathrm{Re}[\hat{\Sigma}^{SL}_{ii}(m^2_{\tilde{\chi}_i}) + \hat{\Sigma}^{SR}_{ii}(m^2_{\tilde{\chi}_i})] \\ & = 0. \end{aligned} \tag{12}$$

Note that we define the coefficients $\Sigma^{L/R}_{ij}(p^2)$ and $\Sigma^{SL/SR}_{ij}(p^2)$ of the self energy via

$$\Sigma_{ij}(p^2) = \not{p} P_L \Sigma^L_{ij}(p^2) + \not{p} P_R \Sigma^R_{ij}(p^2) + P_L \Sigma^{SL}_{ij}(p^2) + P_R \Sigma^{SR}_{ij}(p^2), \tag{13}$$

and define the left and right handed vector and scalar coefficients, $\hat{\Sigma}^{L/R}_{ij}(p^2)$ and $\hat{\Sigma}^{SL/SR}_{ij}(p^2)$ respectively, of the renormalized self-energy analogously.

As stated earlier, we consider the parameter renormalization as for the complex MSSM, such that our setup is easily adaptable for future extensions. In ref. [15, 19], it was shown that in the CP violating case, the 1-loop corrections to the phases of M_1 and μ, i.e. ϕ_{M_1} and ϕ_μ respectively[1] are UV finite. Therefore we take the approach that these phases can be left unrenormalized. We can then determine the necessary conditions to obtain the absolute values $|M_1|$, $|M_2|$ and $|\mu|$, depending on which three physical masses are chosen to be on-shell. As we have two external charginos, and in order to easily extend our setup to the case of $\tilde{\chi}^+_1\tilde{\chi}^-_2$ production, we assume the NCC scheme with $\tilde{\chi}^0_1$, $\tilde{\chi}^\pm_1$ and $\tilde{\chi}^\pm_2$ on-shell [14–16, 19], such that $i' = 1$ and $i'' = 1$ and 2. Note that in choosing the scheme, it is desirable that the on-shell particles should contain significant bino, wino and higgsino components, in order that the M_1, M_2 and μ parameters are accessible. For the above choice, these conditions are satisfied for all the scenarios defined in sec. 4, in which the lightest neutralino always has a sizeable bino-like component. The parameters in question of the chargino mass matrix can then be renormalized via,

$$\begin{aligned}\delta|M_1| = & -\frac{1}{\mathrm{Re}\,(e^{-i\phi_{M_1}} N^2_{i1})F}\Big((2\mathrm{Re}\,(e^{-i\phi_\mu} N_{i3}N_{i4})\mathrm{Re}\,(U_{j1}V_{j1}) \\ & + \mathrm{Re}\,N^2_{i2}\mathrm{Re}\,(e^{-i\phi_\mu}U_{j2}V_{j2}))C_k + (\mathrm{Re}\,(U_{j1}V_{j1})\mathrm{Re}\,(e^{-i\phi_\mu}U_{k2}V_{k2}) \\ & - \mathrm{Re}\,(e^{-i\phi_\mu}U_{j2}V_{j2})\mathrm{Re}\,(U_{k1}V_{k1}))N_i - (\mathrm{Re}\,N^2_{i2}\mathrm{Re}\,(e^{-i\phi_\mu}U_{k2}V_{k2}) \\ & + 2\mathrm{Re}\,(e^{-i\phi_\mu}N_{i3}N_{i4})\,\mathrm{Re}\,(U_{k1}V_{k1}))C_j\Big), \end{aligned} \tag{14}$$

[1] We adopt the convention that M_2 is real.

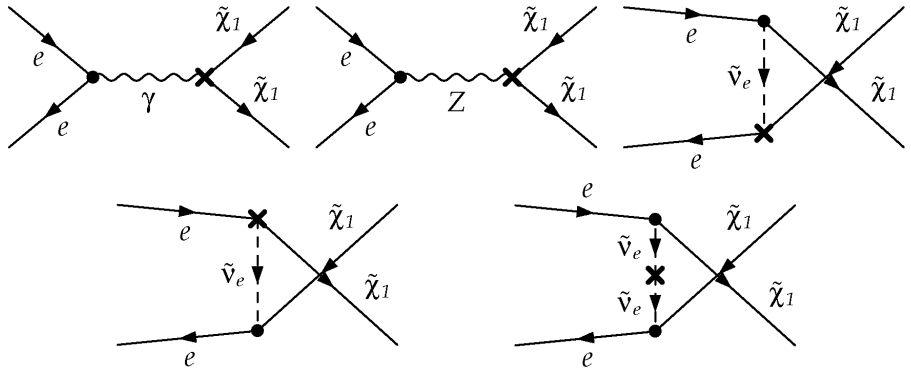

Figure 3: Counterterm diagrams in the MSSM for the production of charginos $\tilde{\chi}_1^+$ and $\tilde{\chi}_1^-$ at the LC.

$$\delta|M_2| = \frac{1}{F}\Big(\mathrm{Re}\,(e^{-i\phi_\mu}U_{j2}V_{j2})C_k - \mathrm{Re}\,(e^{-i\phi_\mu}U_{k2}V_{k2})C_j\Big), \tag{15}$$

$$\delta|\mu| = -\frac{1}{F}\Big(\mathrm{Re}\,(U_{j1}V_{j1})C_k - \mathrm{Re}\,(U_{k1}V_{k1})C_j\Big), \tag{16}$$

where F, C_i and N_i are defined by

$$F = 2\big(\mathrm{Re}\,(U_{k1}V_{k1})\mathrm{Re}\,(e^{-i\phi_\mu}U_{j2}V_{j2}) - \mathrm{Re}\,(U_{j1}V_{j1})\,\mathrm{Re}\,(e^{-i\phi_\mu}U_{k2}V_{k2})\big), \tag{17}$$

$$\begin{aligned} C_i =& \,\mathrm{Re}\,\big[m_{\tilde{\chi}_i^+}[\Sigma^L_{\pm,ii}(m^2_{\tilde{\chi}_i^+}) + \Sigma^R_{\pm,ii}(m^2_{\tilde{\chi}_i^+})] + \Sigma^{SL}_{\pm,ii}(m^2_{\tilde{\chi}_i^+}) + \Sigma^{SR}_{\pm,ii}(m^2_{\tilde{\chi}_i^+})\big] \\ & - \sum_{\substack{j=1,2\\k=1,2}} 2\delta X_{jk}\mathrm{Re}\,(U_{ij}V_{ik}), \end{aligned} \tag{18}$$

$$\begin{aligned} N_i =& \,\mathrm{Re}\,\big[m_{\tilde{\chi}_i^0}[\Sigma^L_{0,ii}(m^2_{\tilde{\chi}_i^0}) + \Sigma^R_{0,ii}(m^2_{\tilde{\chi}_i^0})] + \Sigma^{SL}_{0,ii}(m^2_{\tilde{\chi}_i^0}) + \Sigma^{SR}_{0,ii}(m^2_{\tilde{\chi}_i^0})\big] \\ & - \sum_{\substack{j=1,2\\k=3,4}} 4\delta Y_{jk}\mathrm{Re}\,(N_{ij}N_{ik}), \end{aligned} \tag{19}$$

and the subscripts $\pm$ and 0 identify the coefficients of the chargino and neutralino self-energy respectively.

Finite results for the process of interest at one-loop are obtained by adding the counterterm diagrams shown in fig. 3. Although `FeynArts` generates these diagrams, expressions for the counterterms which renormalize the couplings defined at tree-level in eq. (5) are required as input, and therefore we provide expressions for these here explicitly. For the $\gamma\tilde{\chi}_i^+\tilde{\chi}_j^-$, $Z\tilde{\chi}_i^+\tilde{\chi}_j^-$ and

$e\tilde{\nu}_e\tilde{\chi}_i^+$ vertices, these can be expressed as follows,

$$\delta C^L_{\tilde{\chi}_i^+\tilde{\chi}_j^-\gamma} = C^L_{\tilde{\chi}_i^+\tilde{\chi}_j^-\gamma}\left(\delta Z_e + \frac{\delta Z_{\gamma\gamma}}{2}\right) + C^L_{\tilde{\chi}_i^+\tilde{\chi}_j^- Z}\frac{\delta Z_{Z\gamma}}{2} + \frac{ie}{2}\left(\delta Z^L_{\pm,ij} + \delta\bar{Z}^L_{\pm,ij}\right),$$

$$\begin{aligned}\delta C^L_{\tilde{\chi}_i^+\tilde{\chi}_j^- Z} = {} & C^L_{\tilde{\chi}_i^+\tilde{\chi}_j^- Z}\left(\delta Z_e - \frac{\delta c_W}{c_W} - \frac{\delta s_W}{s_W} + \frac{\delta Z_{ZZ}}{2}\right) + C^L_{\tilde{\chi}_i^+\tilde{\chi}_j^-\gamma}\frac{\delta Z_{\gamma Z}}{2} \\ & - 2ie\frac{\delta s_W}{c_W}\delta_{ij} + \frac{1}{2}\sum_{n=1,2}\left(\delta C^L_{\tilde{\chi}_i^+\tilde{\chi}_n^- Z} Z^L_{\pm,nj} + C^L_{\tilde{\chi}_n^+\tilde{\chi}_j^- Z}\delta\bar{Z}^L_{\pm,in}\right), \quad (20)\end{aligned}$$

where the analogous right-handed parts are obtained by the replacement $L \to R$, and

$$\begin{aligned}\delta C^R_{\tilde{\nu}_e e^+\tilde{\chi}_i^-} = {} & C^R_{\tilde{\nu}_e e^+\tilde{\chi}_i^-}\left(\delta Z_e - \frac{\delta s_W}{s_W} + \frac{1}{2}\left(\delta Z_{\tilde{\nu}_e} + \delta Z_e^{L^*}\right)\right) \\ & + \frac{1}{2}\left(C^R_{\tilde{\nu}_e e^+\tilde{\chi}_1^-}\delta Z^R_{\pm,1i} + C^R_{\tilde{\nu}_e e^+\tilde{\chi}_2^-}\delta Z^R_{\pm,2i}\right). \quad (21)\end{aligned}$$

Note that the renormalization constants of the SM fields, i.e. Z_{VV} $(V = \gamma, Z)$ and δZ_e^L for the vector bosons and electron, and parameters, i.e. δZ_e and $\delta c_W(s_W)$ for the electric charge and cos(sin) of the weak mixing angle respectively, can be found in ref. [19]. The renormalization of the chargino fields are defined in the most general way, making use of separate RCs for the incoming and outgoing fields, i.e. coefficients $\delta Z^{L/R}_{\pm,ij}$ and $\delta\bar{Z}^{L/R}_{\pm,ij}$ respectively for left and right-handed charginos as given in ref. [19]. Finally, the counterterm for the sneutrino self energy, required for the `FeynArts` model file, takes the form

$$\delta C_{\bar{\tilde{\nu}}_i\tilde{\nu}_j} = i\delta_{ij}\left(\frac{1}{2}(\delta Z_{\tilde{\nu}_i} + \delta Z^*_{\tilde{\nu}_i})p^2 - \delta m^2_{\tilde{\nu}_i} - \frac{m^2_{\tilde{\nu}_i}}{2}(\delta Z_{\tilde{\nu}_i} + \delta Z^*_{\tilde{\nu}_i})\right), \quad (22)$$

for $\tilde{\nu}_i = \tilde{\nu}_e$, $\tilde{\nu}_\mu$, $\tilde{\nu}_\tau$, where the sneutrino field and mass RCs, $\delta Z^*_{\tilde{\nu}_i}$ and $\delta m_{\tilde{\nu}_i}$, are also defined following ref. [19].

Inital and final state soft radiation must also be included to obtain an infra-red finite result as the incoming and outgoing particles are charged, and this is done as described in detail in ref. [19], using the phase-space slicing method to define the singular soft and collinear contributions in the regions $E < \Delta E$ and $\theta < \Delta\theta$ respectively. In the soft and collinear limit, regularising using electron and photon masses respectively, these can be factorized into analytically integrable expressions proportional to the tree-level cross-section $\sigma^{\text{tree}}(e^+e^- \to \tilde{\chi}_1^+\tilde{\chi}_1^-)$. However the result is cut-off dependent (i.e. on ΔE

and $\Delta\theta$), and removing this dependence requires a calculation of the cross section for the three body final state, excluding the soft and collinear regions, which can be performed using `FeynArts` and `FormCalc`. It is also possible to include soft photon radiation in the result for the cross-section obtained from `FormCalc`, however the collinear contribution must be added explicitly, for which expressions are given in ref. [19].

4 Fit strategy and numerical results

4.1 Obtaining MSSM parameters from the fit

With the loop corrections calculated as in section 3, we can determine the fundamental parameters of the MSSM at NLO. In the chargino and neutralino sectors there are four real parameters, see sec. 2, which we fit to,

$$M_1, \quad M_2, \quad \mu, \quad \tan\beta\,. \tag{23}$$

Additionally, if the scenario is not such that it would already have been measured at the LC, we fit to the sneutrino mass, as this enters at tree level and will therefore significantly affect cross sections and forward-backward asymmteries. At the loop level, the full MSSM parameter set will contribute. Depending on the scenario, only limited knowledge about some of these may be available. In particular stop sector parameters are likely to be difficult to obtain from LHC data and direct production at the LC might not be possible. However, our analysis also offers unique sensitivity to these parameters at the LC, as stops could significantly contribute to chargino/neutralino observables at NLO.

At the LC, masses are expected to be measured with high precision using different methods [1]. In the following we use the errors which could be achieved using the threshold scan method, however we also investigate how the fit precision changes if the masses were obtained from the continuum. In case of the cross sections, the experimental uncertainty is dominated by the statistical uncertainty [45],

$$\frac{\Delta\sigma}{\sigma} = \frac{\sqrt{S+B}}{S}, \tag{24}$$

where S and B are the signal and background contributions, respectively. In the following, we assume that the statistical uncertainties for the cross sections correspond to an integrated luminosity of $\mathcal{L} = 200$ fb^{-1} per polarisation assuming the efficiency of $\epsilon = 15\%$, which includes branching ratios

for semileptonic final states and selection efficiency of 50% [45]. Similarly, for the forward-backward asymmetry we have

$$\delta(\mathcal{A})_{FB}^{\text{stat}} = \sqrt{\frac{1-\mathcal{A}^2}{N}}, \tag{25}$$

and the total number of events $N = N_+ + N_-$ [45].

In order to estimate the theoretical error, we include the uncertainty due to the contribution of other unknown MSSM parameters, e.g. the heavy pseudoscalar Higgs boson mass m_{A^0}, unless explicitly included in the fit. The other important source of theoretical uncertainty are NNLO corrections. At present, these are only known for chargino and neutralino masses, for which the leading SUSY-QCD NNLO correction was calculated in ref. [39,40]. Based on these results we estimate the uncertainty due to NNLO corrections to be of the order of 0.5 GeV, i.e. comparable to the expected experimental uncertainty. Clearly in the future, NNLO results for cross-sections should ideally be included in order to match the expected experimental uncertainty.

We perform a multi-dimensional χ^2 fit using `Minuit` [46, 47]

$$\chi^2 = \sum_i \left| \frac{\mathcal{O}_i - \bar{\mathcal{O}}_i}{\delta\mathcal{O}_i} \right|^2, \tag{26}$$

where the sum runs over the input observables $\mathcal{O}_i$, depending on the scenario, with their corresponding experimental uncertainties $\delta\mathcal{O}_i$.

4.2 Scenarios studied and motivation

We carry out the fit for three scenarios, S1, S2 and S3, shown in tables 1 and 2. Due to the current status of direct LHC searches [48, 49], in all scenarios we require heavy first and second generation squarks and gluinos. On the other hand the stop sector is assumed to be light, and in fig. 4, for each of these scenarios, the mass corrections for neutralinos $\tilde{\chi}_2^0$ and $\tilde{\chi}_3^0$ are seen to be sensitive to the stop mixing angle. Further, indirect limits lead us to choosing mixed gaugino higgsino scenarios, favoured by the relic density measurements [50] and relatively high pseudoscalar Higgs masses, in light of flavour physics constraints, i.e. the branching ratio $\mathcal{B}(b \to s\gamma)$ and the anomalous magnetic moment of the muon $\Delta(g_\mu - 2)/2$, all of which we checked using `micrOmegas 2.4.1` [51, 52].

Our scenarios are chosen in order to assess the sensitivity to the desired parameters in a number of possible situations. For example, in S2 we study the sensitivity of the fit to large values of M_2, such that the wino-like

Parameter	Value	Parameter	Value
M_1	125	M_2	250
μ	180	M_{A^0}	1000
M_3	700	$\tan\beta$	10
$M_{e_{1,2}}$	1500	M_{e_3}	1500
M_{l_i}	1500	$M_{q_{1,2}}$	1500
M_{q/u_3}	400	A_f	650

Table 1: Table of parameters (with the exception of $\tan\beta$ in GeV), for scenarios 1 (S1) and 2 (S2), where S2 is identical to S1 except $M_2 = 2000$ GeV. Here $M_{(l/q)_i}$ and $M_{(e/u)_i}$ represent the left and right handed mass parameters for of a slepton/squark of generation i respectively, and A_f is the trilinear coupling for a sfermion $\tilde{f}$.

Parameter	Value	Parameter	Value
M_1	106	M_2	212
μ	180	M_{A^0}	500
M_3	1500	$\tan\beta$	12
$M_{e_{1,2}}$	125	M_{e_3}	106
M_{l_i}	180	M_{q_i}	1500
M_{u_3}	450	A_f	-1850

Table 2: Table of parameters (with the exception of $\tan\beta$ in GeV) for scenario 3 (S3).

chargino and neutralino are heavy and decoupled from the bino and higgsino-like particles. Further, in S1/S2 we consider the case that the sleptons and pseudoscalar Higgs bosons are at the TeV scale, and in S3 the case that they are relatively light. Note that S3, see tab. 2, is also chosen to be 125 GeV such that it is compatible with the recent Higgs results from the LHC [53,54].

4.3 Results for scenario 1

In this scenario, only the charginos and three neutralinos will be accessible at the LC. It should be possible to probe the supersymmetric QCD sector, with masses of $\sim$1.5 TeV, at the LHC. As input for the fit we therefore use:

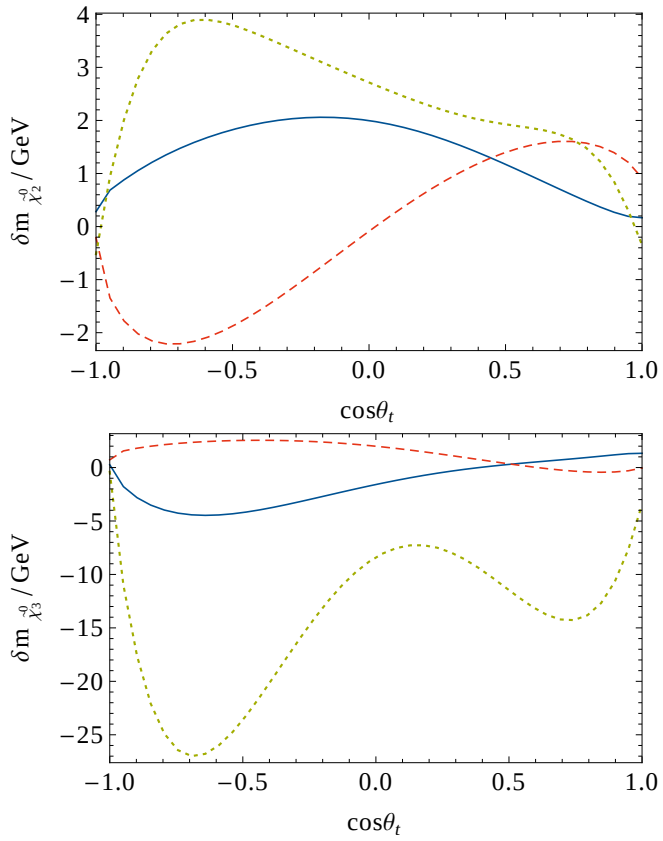

Figure 4: One-loop corrections to the masses of neutralinos $\tilde{\chi}_2^0$ (upper) and $\tilde{\chi}_3^0$ (lower) as a function of the stop mixing angle $\cos\theta_t$, for scenarios S1 (blue), S2 (red, dashed) and S3 (green, dotted).

- the masses of the charginos ($\tilde{\chi}_1^\pm$, $\tilde{\chi}_2^\pm$) and three lightest neutralinos ($\tilde{\chi}_1^0$, $\tilde{\chi}_2^0$, $\tilde{\chi}_3^0$)
- the light chargino production cross section $\sigma(\tilde{\chi}_1^+\tilde{\chi}_1^-)$ with polarised beams at $\sqrt{s} = 350$ and 500 GeV
- the forward-backward asymmetry A_{FB} at $\sqrt{s} = 350$ and 500 GeV
- the branching ratio $\mathcal{B}(b \to s\gamma)$ calculated using `micrOmegas 2.4.1` [51, 52].

The input variables, together with errors are listed in tab. 3. Note that $\mathcal{B}(b \to s\gamma)$ is included in order to increase sensitivity to the third generation squark sector, and the estimated experimental precision of $0.3 \cdot 10^{-4}$, taken

Observable	Tree value	Loop corr.	Error exp.	Error th.
$m_{\tilde{\chi}_1^\pm}$	149.6	–	0.1 (0.2)	–
$m_{\tilde{\chi}_2^\pm}$	292.3	–	0.5 (2)	–
$m_{\tilde{\chi}_1^0}$	106.9	–	0.2	–
$m_{\tilde{\chi}_2^0}$	164.0	2.0	0.5 (1)	0.5
$m_{\tilde{\chi}_3^0}$	188.6	−1.5	0.5 (1)	0.5
$\sigma(\tilde{\chi}_1^+\tilde{\chi}_1^-)^{350}_{(-0.8,0.6)}$	2347.5	−291.3	8.7	2.0
$\sigma(\tilde{\chi}_1^+\tilde{\chi}_1^-)^{350}_{(0.8,-0.6)}$	224.4	7.6	2.7	0.5
$\sigma(\tilde{\chi}_1^+\tilde{\chi}_1^-)^{500}_{(-0.8,0.6)}$	1450.6	−24.4	6.7	2.0
$\sigma(\tilde{\chi}_1^+\tilde{\chi}_1^-)^{500}_{(0.8,-0.6)}$	154.8	12.7	2.0	0.5
$A_{FB}^{350}(\%)$	−2.2	6.8	0.8	0.1
$A_{FB}^{500}(\%)$	−2.6	5.3	1.0	0.1

Table 3: Observables (masses in GeV, cross sections in fb) used as input for the fit in S1, tree-level values and loop corrections are specified. Here the superscript on σ and A_{FB} denotes $\sqrt{s}$ in GeV, and the subscript on σ denotes the beam polarisation $(\mathcal{P}(e^-), \mathcal{P}(e^+))$. The central value of the theoretical prediction, $\mathcal{B}(b \to s\gamma) = 3.3 \cdot 10^{-4}$ GeV, calculated using state-of-the-art tools [51, 52], is also included in the fit. Errors in brackets are for masses obtained from the continuum. See text for details of error estimation.

from ref. [55], is adopted. We found that the impact of the muon anomalous magnetic moment is negligible in this scenario, mainly due to the heavy smuon sector.

In S1 we fit 8 MSSM parameters: M_1, M_2, μ, $\tan\beta$, $m_{\tilde{\nu}}$, $\cos\theta_{\tilde{t}}$, $m_{\tilde{t}_1}$, and $m_{\tilde{t}_2}$. We explicitly check that the impact of other parameters, eg. the masses of the 1st and 2nd generation squarks, is negligible. The small dependence on the A^0 mass is included as an additional source of error. Note that there are no theoretical errors for masses chosen to be on-shell. These masses can be related to the fundamental parameters exactly via tree level relations, and are included in the fit.

The results of the fit are given in tab. 4. We find that the gaugino and higgsino mass parameters are determined with an accuracy better than 1%,

Parameter	Threshold fit		Continuum fit	
M_1	125±0.3	(±0.7)	125±0.6	(±1.2)
M_2	250±0.6	(±1.3)	250±1.6	(±3)
μ	180±0.4	(±0.8)	180±0.7	(±1.3)
$\tan\beta$	10±0.5	(±1)	10±1.3	(±2.6)
$m_{\tilde{\nu}}$	1500±24	$(^{+60}_{-40})$	1500±20	(±40)
$\cos\theta_{\tilde{t}}$	0±0.15	$(^{+0.4}_{-0.3})$	–	
$m_{\tilde{t}_1}$	400^{+180}_{-120}	$(^{\text{at limit}}_{\text{at limit}})$	–	
$m_{\tilde{t}_2}$	800^{+300}_{-170}	$(^{+1000}_{-290})$	800^{+350}_{-220}	$(^{\text{at limit}}_{\text{at limit}})$

Table 4: Fit results (masses in GeV) for S1, for masses obtained from threshold scans (threshold fit) and from the continuum (continuum fit). Numbers in brackets denote 2σ errors.

while $\tan\beta$ is determined with an accuracy of 5%. Excellent precision of 2-3% is obtained for the otherwise unobservable sneutrino. Including NLO effects even allows us to constrain the parameters of the stop sector. Although the precision shown in tab. 4 is rather limited, this could lead to an important hint concerning the masses of the stops, allowing for a well-targeted search at the LHC. This could be another example of LC-LHC interplay [56].

Finally, in tab. 4 we compare the fit results using masses of the charginos and neutralinos obtained from threshold scans and from the continuum. For the latter, the fit quality is seen to deteriorate, with errors on the fundamental parameters almost doubling, clearly indicating the need to measure chargino and neutralino masses via threshold scans.

4.4 Results for scenario 2

In this scenario, where the M_2 parameter is set to 2 TeV, only the light chargino and three lightest neutralinos will be accessible at the LC. As input for the fit we therefore use:

- the masses of the lighter chargino ($\tilde{\chi}_1^{\pm}$) and neutralinos ($\tilde{\chi}_1^0, \tilde{\chi}_2^0, \tilde{\chi}_3^0$)
- the light chargino production cross section $\sigma(\tilde{\chi}_1^+\tilde{\chi}_1^-)$ with polarised beams at $\sqrt{s} = 400$ and 500 GeV

Observable	Tree value	Loop corr.	Error exp.	Error th.
$m_{\tilde{\chi}_1^\pm}$	179.1	–	0.1	–
$m_{\tilde{\chi}_1^0}$	111.1	–	0.2	–
$m_{\tilde{\chi}_2^0}$	183.6	0.07	0.5	0.5
$m_{\tilde{\chi}_3^0}$	194.2	1.9	0.5	0.5
$\sigma(\tilde{\chi}_1^+\tilde{\chi}_1^-)^{400}_{(-0.8,0.6)}$	1214.9	−344.7	6.0	0.1
$\sigma(\tilde{\chi}_1^+\tilde{\chi}_1^-)^{400}_{(0.8,-0.6)}$	250.6	−32.4	2.7	0.1
$\sigma(\tilde{\chi}_1^+\tilde{\chi}_1^-)^{500}_{(-0.8,0.6)}$	1079.2	−194.8	6.0	0.1
$\sigma(\tilde{\chi}_1^+\tilde{\chi}_1^-)^{500}_{(0.8,-0.6)}$	229.6	−8.7	2.7	0.1
$A_{FB}^{400}(\%)$	0.0	3.0	1.0	0.1
$A_{FB}^{500}(\%)$	0.0	5.0	1.0	0.1

Table 5: Observables (masses in GeV, cross sections in fb) used as an input for the fit in S2, as in tab. 5. The central value of the theoretical prediction, $\mathcal{B}(b \to s\gamma) = 3.3 \cdot 10^{-4}$ GeV, calculated using state-of-the-art tools [51, 52], is also included in the fit. See text for details of error estimation.

- the forward-backward asymmetry A_{FB} at $\sqrt{s} = 400$ and 500 GeV
- the branching ratio $\mathcal{B}(b \to s\gamma)$.

As we again find that the muon anomalous magnetic moment has a negligible impact, it is not used in the fit. The input variables, together with errors are listed in tab. 5.

We again fit 8 MSSM parameters: M_1, M_2, μ, $\tan\beta$, $m_{\tilde{\nu}}$, $\cos\theta_{\tilde{t}}$, $m_{\tilde{t}_1}$, and $m_{\tilde{t}_2}$. The impact of other parameters, except the heavy Higgs boson mass, can be neglected. The results from the fit are given in tab. 6. The higgsino and bino mass parameters are well constrained in this scenario since bino-like neutralino and all higgsinos are directly accessible. Even though the winos are not directly accessible, the wino mass parameter M_2 can be constrained with 10% accuracy at 1σ level. An accuracy of 20% is achieved for $\tan\beta$, significantly worse than in S1. This can be understood by the fact that the mixing in S2 between chargino states is weak due to M_2 being heavy, and the constraint on $\tan\beta$ is dependent on this mixing. No limits can be derived on the sneutrino mass, due to the Yukawa suppressed coupling of the higgsino-

Parameter	Fit result
M_1	$125^{+0.9}_{-0.6}$ $\left(^{+2.1}_{-1.2}\right)$
M_2	2000 ± 200 $\left(^{+600}_{-400}\right)$
μ	180 ± 0.2 $\left(^{+0.5}_{-0.3}\right)$
$\tan\beta$	10 ± 2 $\left(^{+5}_{-4}\right)$
$m_{\tilde{\nu}}$	unconstrained
$\cos\theta_{\tilde{t}}$	$0^{+0.13}_{-0.09}$ $\left(^{+0.4}_{-0.3}\right)$
$m_{\tilde{t}_1}$	400^{+250}_{-50} $\left(^{+500}_{-80}\right)$
$m_{\tilde{t}_2}$	800^{+300}_{-200} $\left(^{+900}_{-400}\right)$

Table 6: Fit results (with the exception of $\tan\beta$ and $\cos\theta_{\tilde{t}}$ in GeV) for S2, as in tab. 4, where numbers in brackets denote 2σ errors.

like $\tilde{\chi}_1^\pm$ to the electron and sneutrino. We are however, as shown in tab. 6, still able to derive limits on the stop masses and mixing parameter.

4.5 Results for parameters in scenario 3

This final scenario features the richest phenomenology of the studied benchmark scenarios. As input for the fit we therefore use:

- the masses of the charginos ($\tilde{\chi}_1^\pm$, $\tilde{\chi}_2^\pm$) and neutralinos ($\tilde{\chi}_1^0, \tilde{\chi}_2^0, \tilde{\chi}_3^0$)
- the light chargino production cross section $\sigma(\tilde{\chi}_1^+\tilde{\chi}_1^-)$ with polarised beams at $\sqrt{s} = 400$ and 500 GeV
- the forward-backward asymmetry A_{FB} at $\sqrt{s} = 400$ and 500 GeV
- the Higgs boson mass, m_h
- the branching ratio $\mathcal{B}(b \to s\gamma)$
- the anomalous muon magnetic moment

Compared to the previous scenarios, these observables are supplemented by the Higgs boson mass, m_h, calculated using `FeynHiggs 2.9.1` [57–60]. The estimated experimental precision at the LC for m_h, taken from ref. [1], is adopted. We further assume the theoretical uncertainty on the Higgs boson

Observable	Tree value	Loop corr.	Error exp.	Error th.
$m_{\tilde{\chi}_1^\pm}$	139.3	–	0.1	–
$m_{\tilde{\chi}_2^\pm}$	266.2	–	0.5	–
$m_{\tilde{\chi}_1^0}$	92.8	–	0.2	–
$m_{\tilde{\chi}_2^0}$	148.5	2.4	0.5	0.5
$m_{\tilde{\chi}_3^0}$	189.7	−7.3	0.5	0.5
$\sigma(\tilde{\chi}_1^+\tilde{\chi}_1^-)^{400}_{(-0.8,0.6)}$	709.7	−85.1	0.7	–
$\sigma(\tilde{\chi}_1^+\tilde{\chi}_1^-)^{400}_{(0.8,-0.6)}$	129.8	20.0	0.3	–
$\sigma(\tilde{\chi}_1^+\tilde{\chi}_1^-)^{500}_{(-0.8,0.6)}$	560.0	−70.1	0.7	–
$\sigma(\tilde{\chi}_1^+\tilde{\chi}_1^-)^{500}_{(0.8,-0.6)}$	97.1	16.4	0.3	–
$A_{FB}^{400}(\%)$	24.7	−2.8	1.4	0.1
$A_{FB}^{500}(\%)$	39.2	−5.8	1.5	0.1

Table 7: Observables (masses in GeV, cross sections in fb) used as an input for the fit in S3, as in tab. 3. The central theoretical predictions $\mathcal{B}(b \to s\gamma) = 2.7 \cdot 10^{-4}$, $\Delta(g_\mu - 2)/2 = 2.4 \cdot 10^{-9}$ and $m_h = 125$ GeV, calculated using state-of-the-art tools [51, 52, 57–60], are also included in the fit. See text for details of error estimation.

mass to be 1 GeV [60]. As before, the remaining two observables, the branching ratio $\mathcal{B}(b \to s\gamma)$ and the anomalous muon magnetic moment are calculated using `micrOmegas 2.4.1` [51, 52], and a projected experimental error on the anomalous muon magnetic moment of $3.4 \cdot 10^{-10}$ is employed [61], which we assume would dominate over the theoretical uncertainty. The input variables, along with errors, are summarised in tab. 7. Because the sneutrino is now directly accessible, we assume that its mass has been measured.

In addition to the 7 MSSM parameters fitted in scenarios 1 and 2: M_1, M_2, μ, $\tan\beta$, $\cos\theta_{\tilde{t}}$, $m_{\tilde{t}_1}$, and $m_{\tilde{t}_2}$, we now explicitly include the heavy Higgs boson mass in the fit and remove the sneutrino mass. The results of the fit are collected in tab. 8. The parameters of the electroweak gaugino-higgsino sector are determined with high precision. Due to a significant mixing in the stop sector, and the improvement in the fit quality due to the inclusion of the higgs mass, we find that the fit is now also sensitive to the mass of the heavy,

Parameter	Fit result
M_1	106 ± 0.3 (± 0.5)
M_2	212 ± 0.5 (± 1.0)
μ	180 ± 0.4 (± 0.9)
$\tan\beta$	12 ± 0.3 (± 0.7)
$\cos\theta_{\tilde{t}}$	$0.15^{+0.08}_{-0.06}$ $(^{+0.16}_{-0.09})$
$m_{\tilde{t}_1}$	430^{+200}_{-130} $(^{+300}_{-400})$
$m_{\tilde{t}_2}$	1520^{+200}_{-300} $(^{+300}_{-400})$
m_{A^0}	< 650 (< 1000)

Table 8: Fit results (with the exception of $\tan\beta$ and $\cos\theta_{\tilde{t}}$ in GeV) for S3, as in tab. 4, but in addition including results for the masses of the heavier stop mass ($m_{\tilde{t}_2}$) and the pseudoscalar higgs boson (m_{A^0}).

left-handed stop. The accuracy is better than 20% for this particle even though it is far beyond the reach of the LC and also LHC. In addition, an upper limit on the mass of the heavy Higgs boson can be placed at 1000 GeV, at the 2σ level.

5 Conclusion

The evidence for the Higgs boson and dark matter, when examined in the context of supersymmetry, suggest the possibility of a light μ and M_1. We have extended previous analyses, which fitted observables for chargino production at the LC to extract fundamental MSSM parameters, by incorporating NLO corrections. The loop corrections are calculated for all observables fitted, namely the polarised cross-sections and forward backward asymmetry for chargino production as well as the $\tilde{\chi}_1^\pm, \tilde{\chi}_2^\pm$ and $\tilde{\chi}_1^0, \tilde{\chi}_2^0, \tilde{\chi}_3^0$ masses, in an on-shell scheme which facilitates the extension to the complex case. We have fitted these observables for three complementary scenarios. We found that on including NLO corrections, when M_1, M_2 and μ are light they can be determined to percent-level accuracy, and $\tan\beta$ to $< 5\%$. Further we showed that obtaining masses of the charginos and neutralinos from the continuum as opposed to threshold scans would result in the uncertainty on the funda-

mental parameters almost doubling, reinforcing the importance of threshold scans for mass measurements. As a heavy M_2 is still a viable possibility, we also considered $M_2 = 2000$ GeV, and found that the sensitivity to M_2 is approximately 10%. As the error on $\tan\beta$ is dependent on the degree of mixing in the chargino sector, here it increases to $\sim 20\%$. Note that the inclusion of $\mathcal{B}(b \to s\gamma)$, as well as the use of masses determined via threshold scanning, in the fit was seen to improve the sensitivity to the stop sector. We finally considered a scenario compatible with the latest Higgs results. For this scenario we found that including $\mathcal{B}(b \to s\gamma)$, $\Delta(g_\mu - 2)/2$ and m_h in the fit, along with the significant mixing in the stop sector, helped to obtain an accuracy better than 20% on the mass of the heavy, left-handed stop, even though this particle is far beyond the reach of the LC and also the LHC. We also included m_{A^0} in the fit, and found that it would be possible to place a 2σ upper bound on this parameter of 1000 GeV. In summary, we have shown that incorporating NLO corrections is required for the precise determination of the fundamental parameters of the chargino and neutralino sector at the LC, and could further provide sensitivity to the parameters describing particles which contribute via loop corrections.

Acknowledgements

The authors gratefully acknowledge support of the DFG through the grant SFB 676, "Particles, Strings, and the Early Universe", as well as the Helmholtz Alliance, "Physics at the Terascale". This work was also partially supported by the Polish National Science Centre under research grant DEC-2011/01/M/ST2/02466 and the MICINN, Spain, under contract FPA2010-17747; Consolider-Ingenio CPAN CSD2007- 00042. KR thanks as well the Comunidad de Madrid through Proyecto HEPHACOS S2009/ESP-1473 and the European Commission under contract PITN-GA-2009-237920.

References

[1] **ECFA/DESY LC Physics Working Group** Collaboration, J. Aguilar-Saavedra et al. `hep-ph/0106315`.

[2] **ILC Collaboration** Collaboration, E. Brau, James et al. `arXiv:0712.1950`.

[3] **ILC** Collaboration, G. Aarons et al. `arXiv:0709.1893`.

[4] H. Goldberg *Phys.Rev.Lett.* **50** (1983) 1419.

[5] J. R. Ellis, J. Hagelin, D. V. Nanopoulos, K. A. Olive, and M. Srednicki *Nucl.Phys.* **B238** (1984) 453–476.

[6] L. J. Hall, D. Pinner, and J. T. Ruderman *JHEP* **1204** (2012) 131, [arXiv:1112.2703].

[7] F. Brummer and W. Buchmuller *JHEP* **1107** (2011) 010, [arXiv:1105.0802].

[8] K. Desch, J. Kalinowski, G. A. Moortgat-Pick, M. Nojiri, and G. Polesello *JHEP* **0402** (2004) 035, [hep-ph/0312069].

[9] W. Oller, H. Eberl, and W. Majerotto *Phys.Rev.* **D71** (2005) 115002, [hep-ph/0504109].

[10] T. Fritzsche and W. Hollik *Nucl.Phys.Proc.Suppl.* **135** (2004) 102–106, [hep-ph/0407095].

[11] W. Kilian, J. Reuter, and T. Robens *Eur.Phys.J.* **C48** (2006) 389–400, [hep-ph/0607127].

[12] T. Robens, J. Kalinowski, K. Rolbiecki, W. Kilian, and J. Reuter *Acta Phys.Polon.* **B39** (2008) 1705–1714, [arXiv:0803.4161].

[13] T. Fritzsche. PhD thesis, Universitaet Karlsruhe, 2005.

[14] A. Fowler and G. Weiglein *JHEP* **1001** (2010) 108, [arXiv:0909.5165].

[15] A. Fowler. PhD thesis, Durham University, 2010.

[16] A. Chatterjee, M. Drees, S. Kulkarni, and Q. Xu arXiv:1107.5218.

[17] H. E. Haber and G. L. Kane *Phys.Rept.* **117** (1985) 75–263.

[18] S. Choi, A. Djouadi, M. Guchait, J. Kalinowski, H. Song, et al. *Eur.Phys.J.* **C14** (2000) 535–546, [hep-ph/0002033].

[19] A. Bharucha, A. Fowler, G. Moortgat-Pick, and G. Weiglein arXiv:1211.3134.

[20] J. Kublbeck, M. Bohm, and A. Denner *Comput.Phys.Commun.* **60** (1990) 165–180.

[21] A. Denner, H. Eck, O. Hahn, and J. Kublbeck *Nucl.Phys.* **B387** (1992) 467–484.

[22] J. Kublbeck, H. Eck, and R. Mertig *Nucl.Phys.Proc.Suppl.* **29A** (1992) 204–208.

[23] T. Hahn *Comput.Phys.Commun.* **140** (2001) 418–431, [hep-ph/0012260].

[24] T. Hahn and C. Schappacher *Comput.Phys.Commun.* **143** (2002) 54–68, [hep-ph/0105349].

[25] T. Hahn and M. Perez-Victoria *Comput.Phys.Commun.* **118** (1999) 153–165, [hep-ph/9807565].

[26] T. Hahn *Comput.Phys.Commun.* **178** (2008) 217–221, [hep-ph/0611273].

[27] T. Hahn and M. Rauch *Nucl.Phys.Proc.Suppl.* **157** (2006) 236–240, [hep-ph/0601248].

[28] W. Siegel *Phys.Lett.* **B84** (1979) 193.

[29] W. Siegel *Phys.Lett.* **B94** (1980) 37.

[30] D. Stockinger *JHEP* **0503** (2005) 076, [hep-ph/0503129].

[31] F. del Aguila, A. Culatti, R. Munoz Tapia, and M. Perez-Victoria *Nucl.Phys.* **B537** (1999) 561–585, [hep-ph/9806451].

[32] A. Lahanas, K. Tamvakis, and N. Tracas *Phys.Lett.* **B324** (1994) 387–396, [hep-ph/9312251].

[33] D. Pierce and A. Papadopoulos *Phys.Rev.* **D50** (1994) 565–570, [hep-ph/9312248].

[34] D. Pierce and A. Papadopoulos *Nucl.Phys.* **B430** (1994) 278–294, [hep-ph/9403240].

[35] H. Eberl, M. Kincel, W. Majerotto, and Y. Yamada *Phys.Rev.* **D64** (2001) 115013, [hep-ph/0104109].

[36] T. Fritzsche and W. Hollik *Eur.Phys.J.* **C24** (2002) 619–629, [hep-ph/0203159].

[37] W. Oller, H. Eberl, W. Majerotto, and C. Weber *Eur.Phys.J.* **C29** (2003) 563–572, [hep-ph/0304006].

[38] M. Drees, W. Hollik, and Q. Xu *JHEP* **0702** (2007) 032, [hep-ph/0610267].

[39] R. Schofbeck and H. Eberl *Phys.Lett.* **B649** (2007) 67–72, [hep-ph/0612276].

[40] R. Schofbeck and H. Eberl *Eur.Phys.J.* **C53** (2008) 621–626, [arXiv:0706.0781].

[41] K. Rolbiecki and J. Kalinowski *Phys.Rev.* **D76** (2007) 115006, [arXiv:0709.2994].

[42] H. Eberl, T. Gajdosik, W. Majerotto, and B. Schrausser *Phys.Lett.* **B618** (2005) 171–181, [hep-ph/0502112].

[43] P. Osland and A. Vereshagin *Phys.Rev.* **D76** (2007) 036001, [arXiv:0704.2165].

[44] A. Bharucha, S. Heinemeyer, F. von der Pahlen, and C. Schappacher arXiv:1208.4106.

[45] K. Desch, J. Kalinowski, G. Moortgat-Pick, K. Rolbiecki, and W. Stirling *JHEP* **0612** (2006) 007, [hep-ph/0607104].

[46] F. James and M. Roos *Comput.Phys.Commun.* **10** (1975) 343–367.

[47] F. James *CERN Program Library Long Writeup D506* (1994).

[48] **ATLAS Collaboration** Collaboration, G. Aad et al. arXiv:1208.0949.

[49] **CMS Collaboration** Collaboration, S. Chatrchyan et al. arXiv:1207.1798.

[50] **WMAP Collaboration** Collaboration, E. Komatsu et al. *Astrophys.J.Suppl.* **192** (2011) 18, [arXiv:1001.4538].

[51] G. Belanger, F. Boudjema, A. Pukhov, and A. Semenov *Comput.Phys.Commun.* **176** (2007) 367–382, [hep-ph/0607059].

[52] G. Belanger, F. Boudjema, P. Brun, A. Pukhov, S. Rosier-Lees, et al. *Comput.Phys.Commun.* **182** (2011) 842–856, [arXiv:1004.1092].

[53] **ATLAS Collaboration** Collaboration, G. Aad et al. *Phys.Lett.* **B716** (2012) 1–29, [arXiv:1207.7214].

[54] **CMS Collaboration** Collaboration, S. Chatrchyan et al. *Phys.Lett.* **B716** (2012) 30–61, [arXiv:1207.7235].

[55] **SuperB Collaboration** Collaboration, B. O'Leary et al. arXiv:1008.1541.

[56] **LHC/LC Study Group** Collaboration, G. Weiglein et al. *Phys.Rept.* **426** (2006) 47–358, [hep-ph/0410364].

[57] S. Heinemeyer, W. Hollik, and G. Weiglein *Comput.Phys.Commun.* **124** (2000) 76–89, [hep-ph/9812320].

[58] S. Heinemeyer, W. Hollik, and G. Weiglein *Eur.Phys.J.* **C9** (1999) 343–366, [hep-ph/9812472].

[59] G. Degrassi, S. Heinemeyer, W. Hollik, P. Slavich, and G. Weiglein *Eur.Phys.J.* **C28** (2003) 133–143, [hep-ph/0212020].

[60] M. Frank, T. Hahn, S. Heinemeyer, W. Hollik, H. Rzehak, et al. *JHEP* **0702** (2007) 047, [hep-ph/0611326].

[61] R. Carey, K. Lynch, J. Miller, B. Roberts, W. Morse, et al.